



Harmonic effects optimization at a system level using a harmonic power flow controller

Reza MEHRI¹ , Hossein MOKHTARI^{2,*} 

¹Department of Engineering, College of Electrical Engineering, Tehran Science and Research Branch, Islamic Azad University, Tehran, Iran

²Department of Electrical Engineering, Sharif University of Technology, Tehran, Iran

Received: 27.11.2018

Accepted/Published Online: 03.04.2020

Final Version: 25.09.2020

Abstract: Increase of nonlinear loads in industries has resulted in high levels of harmonic currents and consequently harmonic voltages in power networks. Harmonics have several negative effects such as higher energy losses and equipment life reduction. To reduce the levels of harmonics in power networks, different methods of harmonic suppression have been employed. The basic idea in all of these methods is to prevent harmonics from flowing into a power network at customer sides and the point of common coupling (PCC). Due to the costs, none of the existing mitigating methods result in a harmonic-free power system. The remaining harmonic currents, which rotate in a power network according to the system impedances, may not necessarily result in an optimum harmonic power flow in terms of harmonic undesirable results such as harmonic losses or harmonic over voltage/current due to possible resonances. This paper proposes a new method to control the flow of the remaining harmonics at a power system level such that the effects of harmonics such as losses are optimized. This task is achieved by the use of series active power filters controlled in a different manner from their conventional methods. In this new application, the series active power injects a controlled harmonic voltage into a power system (e.g., a line, transformer, or other elements) to control the harmonic current (power) flow such that the overall performance of the power system is improved in terms of harmonic effects. The series active power filter in this new application is named as harmonic power flow controller (HPFC). In this paper, the theory, structure, applications, and the basics of the control method of a HPFC are described. To investigate the effects of the HPFC on the power network harmonics, an HPFC is used in the 14-busbar IEEE test system. To make the proposal more practical, an HPFC is designed for Iran north-west transmission system to alleviate the harmonic problem in this region. Simulations are carried out to show the effectiveness of the HPFC. Simulation results show that the HPFC can control the harmonic currents (power) and voltage consequently. In this paper, several control algorithms for an HPFC are also considered to achieve the desired harmonic voltages levels.

Key words: Current harmonic flow, harmonic power flow controller, harmonic voltage control, minimum apparent power injection, zero active power injection

1. Introduction

Harmonic currents and voltages have been increasing in power networks due to the increase of nonlinear loads in electrical networks. Increase of harmonic in power systems has caused several effects such as inefficient performance, lifespan reduction and performance failures in the elements of a power system such as transformers

*Correspondence: mokhtari@sharif.edu

and capacitor banks. Additionally, the increase of harmonics results in higher losses in electrical equipment and may cause large voltages/currents due to possible parallel/series resonances.

Several solutions have been proposed to attenuate harmonics in power networks. Structural considerations, network regulations, development of equipment with low supply current distortion and installation of harmonic suppressors are different levels of distortion prevention methods [1]. Active and passive harmonic filters are used to mitigate current and voltage harmonics [2–5]. They are normally connected at load buses in order to achieve the best harmonic mitigation [6–9]. Although, engineers try to mitigate harmonics as much as possible, they are still present in power distribution/transmission networks for the following reasons.

1. Some sources of harmonics are domestic/commercial loads which share a distribution transformer. In such cases, normally no harmonic filters are used.

2. While large industries tend to use harmonic filters, small-scale industries may not be interested in investing on harmonic-mitigating equipment considering the fact that they are not forced to pay for the harmonic currents losses. Also, parts of the harmonics in power systems are due to large quantities of low power loads such as CPFLs whose cumulative harmonic effects appear at high voltage levels.

3. Even in case of using harmonic-mitigating equipment, the level of harmonic currents/voltages are reduced to a standard level. Therefore, the upstream network will never be harmonic free [10,11].

4. The injected harmonics into a distribution/transmission network cannot be easily absorbed by shunt harmonic filters due to the high short circuit levels in such networks [2].

The remaining harmonics in distribution/transmission networks flow according to the network series or parallel impedances, and therefore, no direct control exists on the harmonic flows.

As a consequence, harmonic losses may not be minimized in the system due to the fact that both line resistance and reactance affect the harmonic current flow. It can also be concluded that lines reactances play a more important role than lines resistances because a) normally in distribution systems and especially in transmission systems, the reactance term is larger than the resistive term, and b) the rate of the increase of an inductive impedance due to the increase of harmonic orders is higher than that in a resistive impedance (skin effect).

The conclusion is that uncontrolled flow of the remaining harmonic currents in upstream networks may not result in either an optimum operation of the system from the efficiency point of view or from a safe operation of the equipment. The question now is "can we force the remaining harmonic currents in power systems to flow in a desired way such that the harmonic effects in the power system (losses or equipment insulation failures) are minimized?" This paper, for the first time, proposes a new application for series active power filters to answer that question. Series active filters have been already used to reduce harmonic at a source side. The difference is that now, a voltage harmonic term is deliberately injected by the filter into a network to force the harmonic currents to flow through a desired direction. Therefore, the series active power filter plays the role of a harmonic power flow controller or HPFC. One can also think HPFC as a harmonic phase shifter as compared to a conventional phase shifter. A phase shifter controls a power flow at the fundamental frequency, while an HPFC controls a power flow at a harmonic frequency.

The structure of this paper is as follows: In Section 2, the structure and configuration of an HPFC is presented. Section 3 studies the performance of an HPFC and investigates its effect on the system harmonic voltage and power losses. The test system is the IEEE 14-bus test bed. The effect of the injected harmonic signal on the objective function is also studied in this section. In Section 4, the basics of the control methods

that are applicable to an HPFC are described. Section 5 designs an HPFC system for a real harmonic problem in Iran north-west transmission system. All the simulations are carried out by MATLAB and DIGSILENT softwares. Finally, Section 6 summarizes the conclusions.

2. HPFC fundamentals and structure

To control the flow of current harmonics in a nonradial or a loop network, an HPFC needs to have the capability of (i) controlling the magnitude and the angle of the series injected harmonic voltage, and (ii) measuring the current and voltage harmonics of the series element. Therefore, an HPFC can be considered as a series static converter that detects the current harmonics and injects a suitable voltage harmonic via a series transformer. Figure 1a shows a circuit diagram of an HPFC on a sample line. The HPFC is composed of three parts; a voltage source converter (VSC), an energy storage element, and a series transformer. In this configuration, the voltage harmonic term is generated by the VSC and injected through the series transformer into the grid. It can be seen from Figure 1a that an HPFC has the same power circuit configuration as a series active filter or a dynamic voltage restorer (DVR) [12], but operated with a different control strategy.

Similar to the presag/in-phase control of a DVR, an HPFC can be controlled in such a way that an active power is exchanged between the HPFC and the system. Note that in the case of an HPFC, the injected voltage is a harmonic term, and therefore, the exchange of power occurs at a harmonic frequency. In this case, the size of the HPFC may be minimum, but the dc link of the HPFC needs to have an energy storage system or have a configuration shown in Figure 1b.

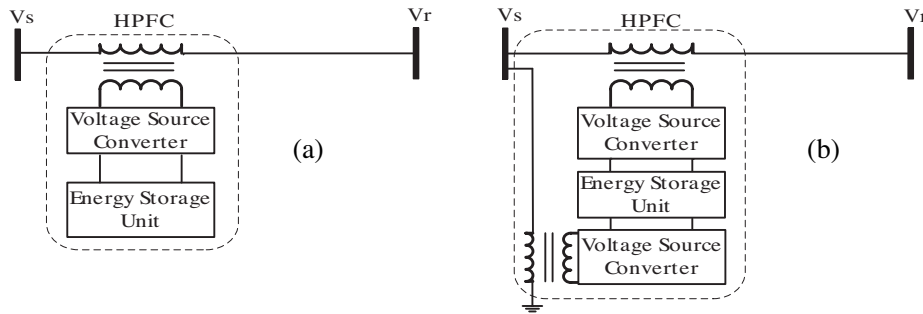


Figure 1. HPFC circuit diagram on a sample line, a) without active power exchange, b) with active power exchange.

If an HPFC is controlled such that no active power is exchanged between the HPFC and the grid, no energy storage system or no extra VSC is required. This can be compared to the energy-minimized compensation method of a DVR. In this method, no energy storage is needed, but the size of the HPFC is not minimal.

For conceptual and steady-state analysis, the HPFC is an application of a series active power filter that is modeled as a series harmonic voltage source whose amplitude and angle are controllable. Figure 2 shows an equivalent model of the HPFC. In this model, the amplitude and the angle of line current harmonic (I_h) can be controlled by the amplitude (V_{hpfc}) and angle (θ_h) of the HPFC output.

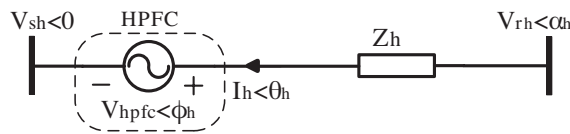


Figure 2. HPFC equivalent model with no active power exchange with the network.

3. HPFC conceptual performance study

This section tries to conceptually show that the HPFC proposed idea is feasible. The detailed control algorithm is described in the next section. To study the performance of the HPFC conceptually, an HPFC is located on an IEEE 14-busbar test system [1,10,12]. Figure 3 shows the system under study. The study is performed for only the 5th harmonic which is normally the dominant harmonic in power networks. Clearly, the proposed concept can be extended to other order harmonics or even combination of several harmonics.

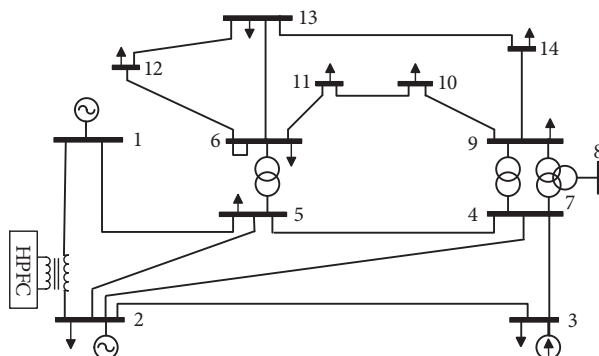


Figure 3. The 14 busbar test system, an HPFC, and the harmonic source [8].

As Figure 3 shows, an HPFC is placed in the feeder between buses 1 and 2. It is worth nothing that finding the minimum number of HPFCs and their best locations to acheive the best harmonic flow solution require an extensive work which cannot be included in this paper, and are left for future studies. Table 1 lists the values of the linear and nonlinear loads in the system. Figure 4 shows the 5th harmonic content in the system under study at normal conditions when an HPFC is employed. The HPFC injects a 5th harmonic voltage (V_{hpfc}) in the line between buses 1 and 2. The amplitude of the injected voltage is changed from 0.2% to 1%, and the angle of the injected signal is changed from 0° to 360° .

Table 1. Specification of the 5th harmonic loads under study [8].

Bus No.	4	5	8	9	10	11	12	13	14
Mag. (%)	10	20	20	15	10	25	20	15	20
Angle ($^\circ$)	5	10	30	10	80	50	30	20	30

Figure 4 shows the harmonic current in the same line, and Figure 5 shows the 5th harmonic voltage at bus 1 as the result of the inclusion of the HPFC. The results show that the voltage and the current harmonic values can be controlled by the amplitude and angle of the HPFC.

Figures 6 and 7 show the active and reactive powers flow between the HPFC and the line. It is clear that the flow of harmonic active power depends on the angle and the amplitude of V_{hpfc} . For specific V_{hpfc} angles (135° , 315°) and different HPFC amplitudes, the exchanged harmonic active power is zero.

3.1. Transformer loss and age control

The total losses of a transformer are determined by no-load, copper and stray losses. The stray losses are subdivided into winding stray losses (P_{SL}) and stray loss in the components other than the windings (P_{OSL}).

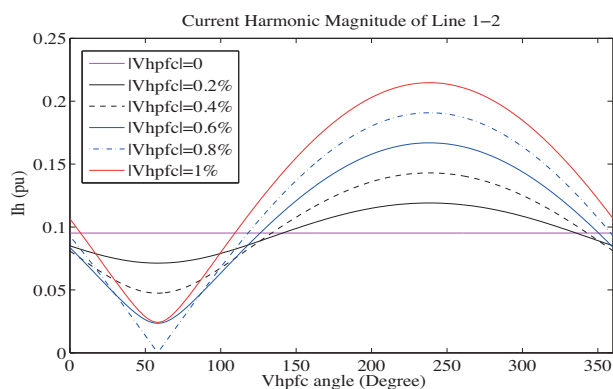


Figure 4. Harmonic current in the HPFC line.

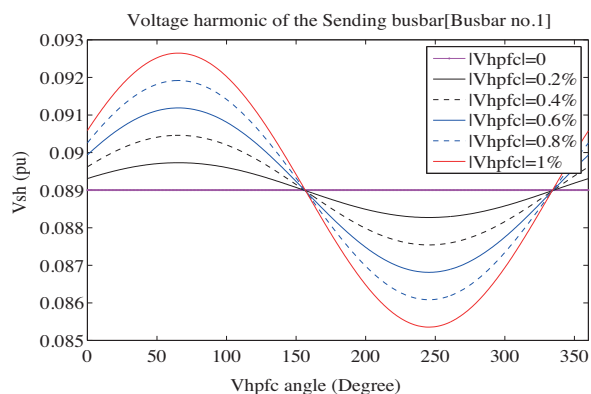


Figure 5. Harmonic voltage at bus no.1.

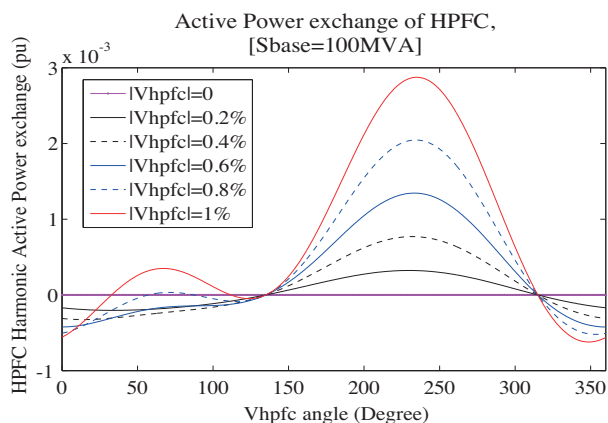


Figure 6. Harmonic active power flow between the HPFC and the line.

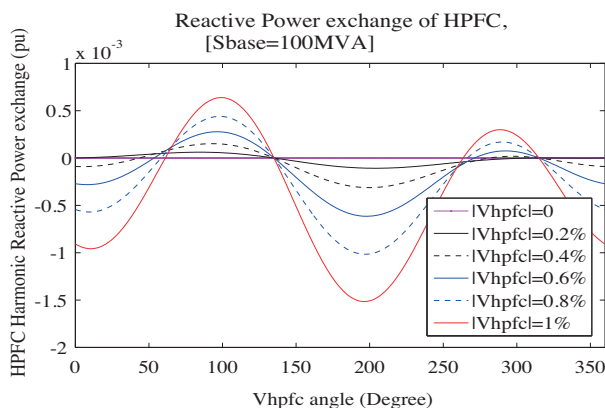


Figure 7. Harmonic reactive power flow between the HPFC and the line.

According to IEEE Std C57.110-1998, harmonic currents flowing through transformers increase the total loss of transformers. P_{SL} and P_{OSL} are proportional to the square of load currents. For a nonsinusoidal load current, P_{SL} increases at a rate proportional to the square of the frequency, but P_{OSL} increases by harmonics with an exponent factor of 0.8 [13, 14]. For liquid-filled transformers, the top oil rise (θ_{TO}) and the conductor hot spot rise (θ_g) will increase as the total load losses increase with harmonic loading. Any increase in other stray losses (P_{OSL}) will primarily affect the top oil rise. It is convenient to define F_{HL} and F_{HL-STR} factors which correspond to the winding eddy losses and other stray losses proportionally. Harmonic loss factor (F_{HL}) is the ratio of the total eddy-current losses due to harmonics, (P_{EC}), to the eddy-current losses at the power frequency when no harmonic currents exist, (P_{EC-0}) [13]. Other harmonic stray loss factor (F_{HL-STR}) is the ratio of the total other stray losses due to harmonics (P_{OSL}) to the total other stray losses at the power frequency when no harmonic currents exist (P_{OSL-R}) [13].

The top oil rise and conductor hot spot rise and hot spot rise in oil-filled transformers may be estimated as a function of, θ_A , which is the ambient temperature of the transformer.

$$\theta_H = \theta_{TO} + \theta_g + \theta_A. \tag{1}$$

The aging acceleration factor (F_{AA}), which shows the rate of the transformer aging acceleration, may be estimated using (2) and (3). The life time of a transformer may be estimated by F_{AA} with respect to the rated life time [15, 16].

$$F_{AA} = \exp\left[\frac{15000}{383} - \frac{15000}{\theta_H + 273}\right]. \tag{2}$$

$$\text{Real life} = \frac{\text{Normal insulating life}}{F_{AA}}. \tag{3}$$

When a current harmonic flows through a transformer, the total hot spot temperature and F_{AA} will increase. When F_{AA} exceeds 1, the transformer real life time will decrease [17].

In the system shown in Figure 3, the HPFC is moved to the transformer between buses 5 and 6. Now, the HPFC injects a 5th harmonic voltage at Bus 5 or 6 side of the transformer. The amplitude of the injected voltage is changed from 0.2% to 1%, and the angle of the signal is changed from 0° to 360°. Figure 8 shows the transformer power losses when an HPFC controls the harmonic current of the transformer. Figures 9 and 10 show the hot spot temperature and the aging variation factor of the transformer due to the HPFC. This simulation shows that by the HPFC, the power loss, the hot spot temperature and the age of the transformer can be affected. When the HPFC injects 1%∠240° harmonic voltage, the hot spot temperature decreases to 110° and F_{AA} decreases to 1. The high values of the injected voltages in Figure 8 are not practical. These values are just used to show the main concept.

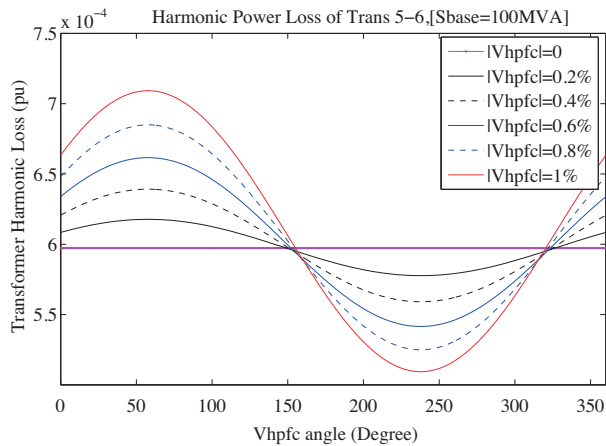


Figure 8. Power loss of transformer 5-6 by the HPFC control.

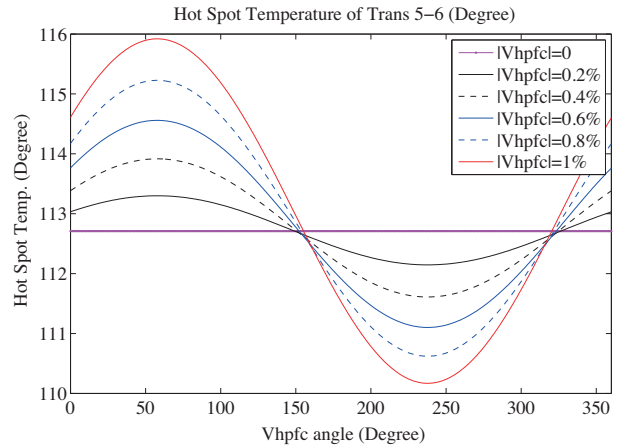


Figure 9. Hot spot temperature of transformer 5-6 by the HPFC control.

The results show that at normal conditions and when no HPFC is used, F_{AA} increases about 30% because of the harmonics. If the HPFC is used properly, the life span reduction of the transformer can be prevented.

4. HPFC control algorithm

The same as a DVR [18,19], the size and complexity of an HPFC depend on the magnitude and phase angle of the series injected harmonic voltage V_{hpfc} . Several harmonic voltage injection strategies can be considered,

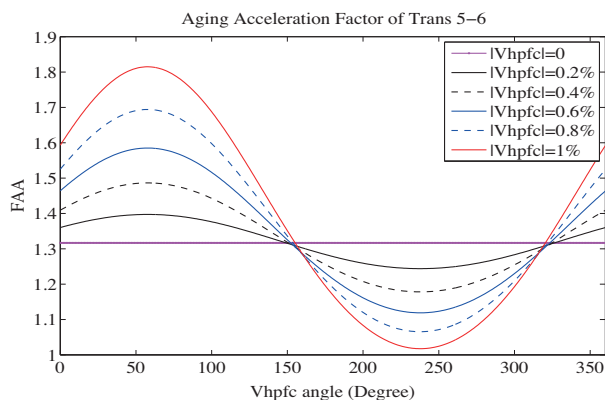


Figure 10. F_{AA} of transformer 5-6 by the HPFC control.

and depending on the active/reactive/harmonic power exchange between the line and the HPFC, the structure and size of the HPFC will change. Since an HPFC may be used in a loop network, it may not be suitable to use the terms load or source side voltage as in the case of a DVR or a series active power filter. Therefore, from now on, the new terms of bus and line sides are used for an HPFC. Figure 11 shows a general block diagram of the control method of the HPFC. It is worth mentioning that in the current manuscript, the performance of the HPFC is evaluated based on an open-loop control strategy. This implies that the harmonic profile of the network is assumed unchanged.

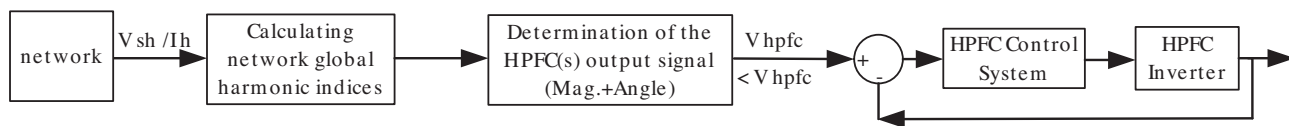


Figure 11. HPFC general control block diagram.

In the following subsections, two control methods are explained. The parameters used in this section are as follows:

- Z_h : Harmonic impedance of the HPFC line,
- V_{sh} : Bus-side harmonic voltage before and after HPFC injection,
- V_{rh0}/V_{rh} : Line-side harmonic voltage before/after HPFC injection,
- I_{h0}/I_h : Line harmonic current before/after HPFC injection, and
- V_{hpfc} : HPFC injected harmonic voltage.

The bus-side harmonic voltage (V_{sh}) is assumed to be unchanged. The injected harmonic voltage V_{hpfc} is such that the magnitude of V_{rh0} before and after the injection remains the same.

4.1. Minimum apparent power (MAPI) method

In this method, the injected harmonic voltage V_{hpfc} is such that the rating of the HPFC is minimized. To achieve this, the injected harmonic voltage (V_{hpfc}) must be as low as possible. This results in an injection signal in-phase with V_{rh} as shown in Figure 12. In this diagram, the dashed-line circle is the locus of V_{rh} considering that $|Z_h \cdot \vec{I}_h + \vec{V}_{hpfc}|$ is constant. The other circle shows the locus of V_{rh} that is the same as V_{rh0} .

It is assumed that θ_h remains constant. For this purpose, the intersection of these curves will be the desired V_{hpfc} . The following derivations based on Figure 12 describe this method.

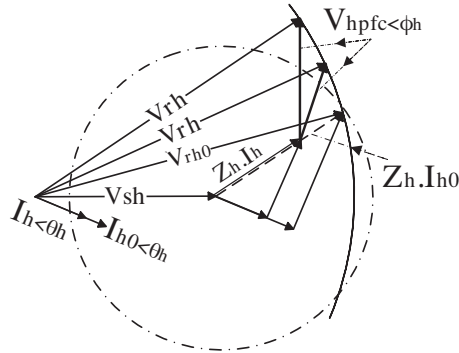


Figure 12. HPFC control vector diagram in MAPI method.

$$\begin{aligned} \vec{V}_{rh} &= \vec{V}_{Sh} + Z_h \cdot \vec{I}_h = V_{Sh} + (R_h + jX_h) I_h (\cos\theta_h + j\sin\theta_h) = \\ & [V_{Sh} + R_h \cdot I_h \cdot \cos\theta_h - X_h \cdot I_h \cdot \sin\theta_h] + j [X_h \cdot I_h \cdot \cos\theta_h + R_h \cdot I_h \cdot \sin\theta_h] . \end{aligned} \tag{4}$$

In these equations, V_{sh} and V_{rh} are the harmonic voltage vectors of the bus-side and line-side respectively. Also, R_h , X_h and Z_h are the resistance, reactance and impedance of the line in which the HPFC is installed. It is assumed that the HPFC decreases the line harmonic current by a factor of K_{hpfc} (%).

$$\begin{aligned} |V_{hpfc}| &= |V_{rho}| - \sqrt{\{ [V_{Sh} + R_h \cdot I_h \cdot \cos\theta_h - X_h \cdot I_h \cdot \sin\theta_h]^2 + [X_h \cdot I_h \cdot \cos\theta_h + R_h \cdot I_h \cdot \sin\theta_h]^2 \}} \\ \alpha_h = \angle V_{hpfc} &= \tan^{-1} \left(\frac{[X_h \cdot I_h \cdot \cos\theta_h + R_h \cdot I_h \cdot \sin\theta_h]}{[V_{Sh} + R_h \cdot I_h \cdot \cos\theta_h - X_h \cdot I_h \cdot \sin\theta_h]} \right) . \end{aligned} \tag{5}$$

Therefore, based on (5), the value and angle of V_{hpfc} can be found as:

$$|V_{hpfc}| = |V_{rho}| - \sqrt{\{ [V_{Sh} + R_h \cdot I_h \cdot \cos\theta_h - X_h \cdot I_h \cdot \sin\theta_h]^2 + [X_h \cdot I_h \cdot \cos\theta_h + R_h \cdot I_h \cdot \sin\theta_h]^2 \}} . \tag{6}$$

$$\alpha_h = \angle V_{hpfc} = \tan^{-1} \left(\frac{[X_h \cdot I_h \cdot \cos\theta_h + R_h \cdot I_h \cdot \sin\theta_h]}{[V_{Sh} + R_h \cdot I_h \cdot \cos\theta_h - X_h \cdot I_h \cdot \sin\theta_h]} \right) . \tag{7}$$

To investigate the effect of the MAPI control method on the performance of the HPFC, an HPFC is installed in line 1-2. In MAPI control method, the magnitude and angle of the injected harmonic voltage depend on the line current harmonic angle. Therefore, in this simulation, the angle of the line current harmonic is changed from 0° to 360° . Figures 13 and 14 show the magnitude and angle of the HPFC signal for different values of K_{hpfc} . The loading of the HPFC is shown in Figure 15. Figure 16 shows the the harmonic active power exchange between the HPFC and the network.

In the MAPI control method, harmonic apparent and active power exchange between the HPFC and line depend on K_{hpfc} . In this method, the HPFC needs a power supply unit to feed the required harmonic active power. In spite of the complexity of the HPFC structure, the rating of the HPFC is minimum.

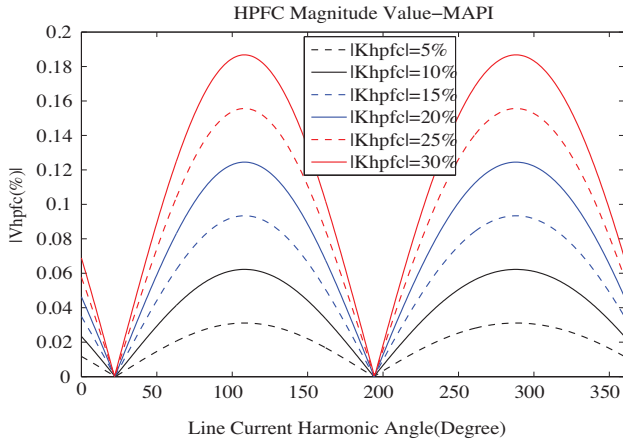


Figure 13. Magnitude of V_{hpfc} for different line current harmonic angles in MAPI control method.

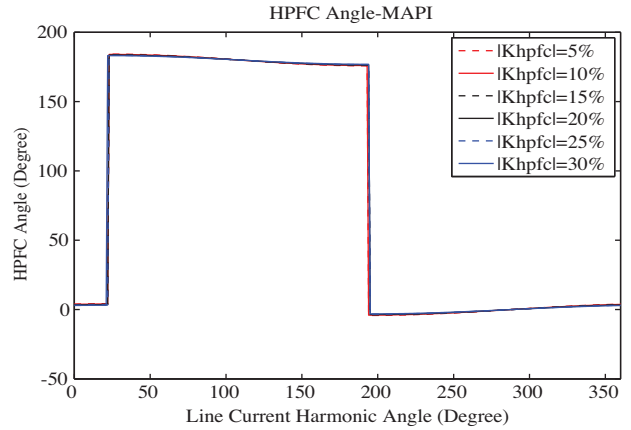


Figure 14. Angle of V_{hpfc} for different line current harmonic angles in MAPI control method.

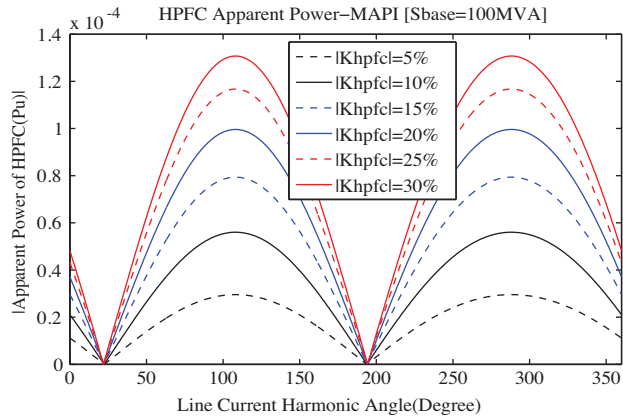


Figure 15. HPFC harmonic apparent power exchange for different line current harmonic angles in MAPI control method.

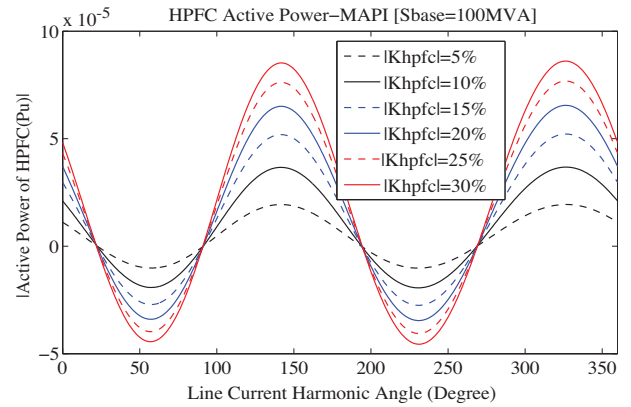


Figure 16. HPFC harmonic active power exchange for different line current harmonic angles in MAPI control method.

4.2. Zero active power (ZAPI) method

Figure 17 shows the vector diagram of the HPFC in the ZAPI control method. In this method, the HPFC injected harmonic voltage V_{hpfc} is perpendicular to the harmonic current. Therefore, no harmonic power is exchanged between the HPFC and the network. The following equations govern the system in this method. When the receiving bus voltage magnitude before and after injection ($V_{rh0} = V_{rh}$) is equal, the HPFC busbar voltage range can be calculated as follows:

$$\vec{V}_{rh0} = \vec{V}_{Sh} + Z_h \cdot \vec{I}_{h0} \tag{8}$$

$$\vec{V}_{rh} = \vec{V}_{Sh} + Z_h \cdot \vec{I}_h + \vec{V}_{hpfc} = V_{Sh} + (R_h + jX_h) I_h (\cos\theta_h + j\sin\theta_h) + jV_{hpfc} = \{ [V_{Sh} + R_h \cdot I_h \cdot \cos\theta_h - X_h \cdot I_h \cdot \sin\theta_h] + j [X_h \cdot I_h \cdot \cos\theta_h + R_h \cdot I_h \cdot \sin\theta_h + V_{hpfc}] \} \tag{9}$$

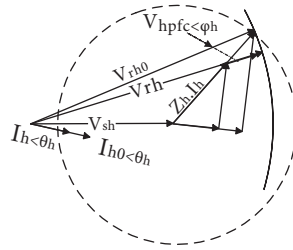


Figure 17. HPFC controlling vector diagram in ZAPI method.

Since $V_{rh} = V_{rh0}$:

$$|V_{rho}| = \left\{ [V_{Sh} + R_h \cdot I_{h0} \cdot \cos\theta_h - X_h \cdot I_{h0} \cdot \sin\theta_h]^2 + [X_h \cdot I_{h0} \cdot \cos\theta_h + R_h \cdot I_{h0} \cdot \sin\theta_h]^2 \right\}^{1/2} = \left\{ [V_{Sh} + R_h \cdot I_h \cdot \cos\theta_h - X_h \cdot I_h \cdot \sin\theta_h]^2 + [X_h \cdot I_h \cdot \cos\theta_h + R_h \cdot I_h \cdot \sin\theta_h + V_{hpfc}]^2 \right\}^{1/2} \tag{10}$$

Solving (10) yields:

$$|V_{hpfc}|^2 + B \cdot |V_{hpfc}| + C = 0 \tag{11}$$

where B and C are:

$$B = 2(X_h \cdot I_h - V_{Sh} \cdot \sin\theta_h) \tag{12}$$

$$C = (R_h \cdot I_h)^2 + (X_h \cdot I_h)^2 - (R_h \cdot I_{h0})^2 + (X_h \cdot I_{h0})^2 + 2 \cdot V_{Sh} \cdot (I_h - I_{h0}) \cdot (R_h \cdot \cos\theta_h - X_h \cdot \sin\theta_h) \tag{13}$$

To investigate the effect of the ZAPI control method on the performance of the HPFC, similar to the MAPI control method, an HPFC is installed in line 1-2. In this control method, the magnitude and angle of the injected voltage harmonic depend on the current harmonic angle. Therefore, the same as the previous control method, the angle of the line current harmonic is changed from 0° to 360°.

Figure 18 shows the variation of the harmonic apparent power flow between the HPFC and the network. Figure 19 shows that active power of the HPFC is negligible. Therefore, in ZAPI, at specific values of the HPFC, the active harmonic power of the HPFC is approximately zero.

In the ZAPI control method, the harmonic apparent power exchange between the HPFC and line depends on K_{hpfc} . In this method, HPFC structure is simple because the active power of the HPFC is approximately zero. However, the rating of the HPFC is higher than it is in the MAPI method.

Figure 20 shows the locus of the amplitude of the HPFC versus its angle in ZAPI control method (HPFC is installed in line 4-7). This figure shows that for ZAPI control method, the amplitude and angle of the HPFC depend on each other.

Figure 21 shows the harmonic apparent/reactive/active power of the HPFC in ZAPI control method. Simulation results show that no active power is exchanged between the HPFC and the network in this method.

Figure 22 shows the HPFC line harmonic current variation and the HPFC harmonic reactive power versus the HPFC amplitude in ZAPI control method. This graphs show that the HPFC amplitude is limited by the degree of harmonic current control and the HPFC capacity.

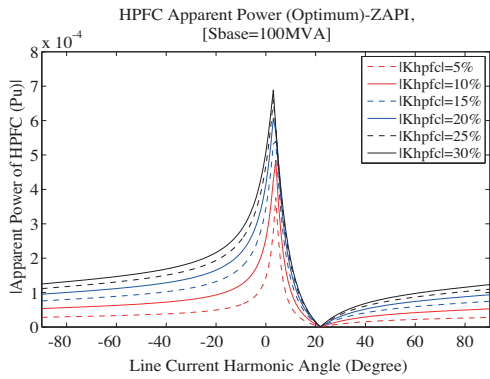


Figure 18. HPFC harmonic apparent power exchange for different line current harmonic angles in ZAPI control method.

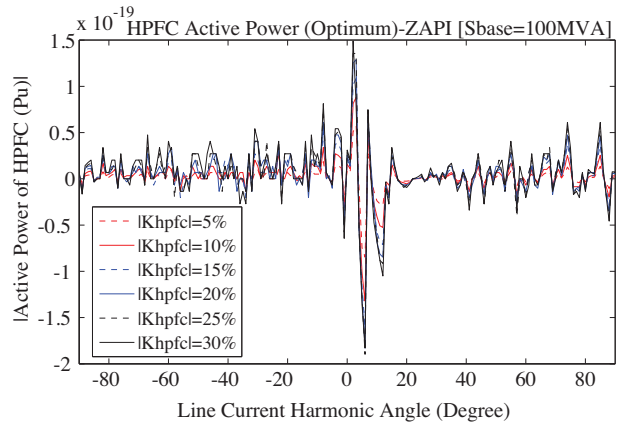


Figure 19. HPFC harmonic active power exchange for different line current harmonic angles in ZAPI control method.

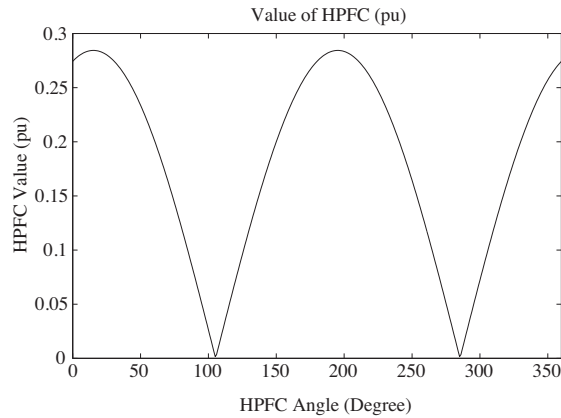


Figure 20. Locus of HPFC amplitude angle in ZAPI control method.

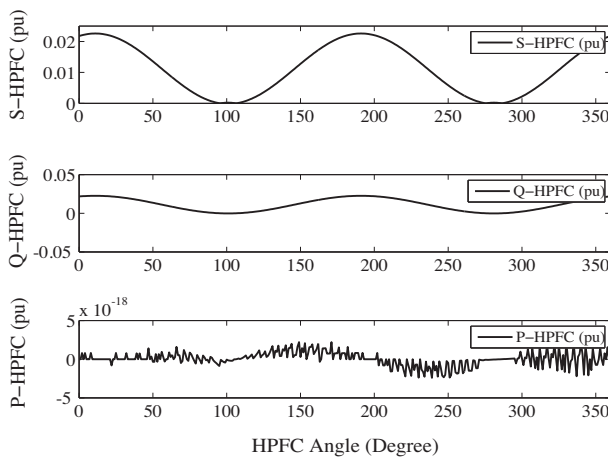


Figure 21. Harmonic apparent, reactive and active power of HPFC in ZAPI.

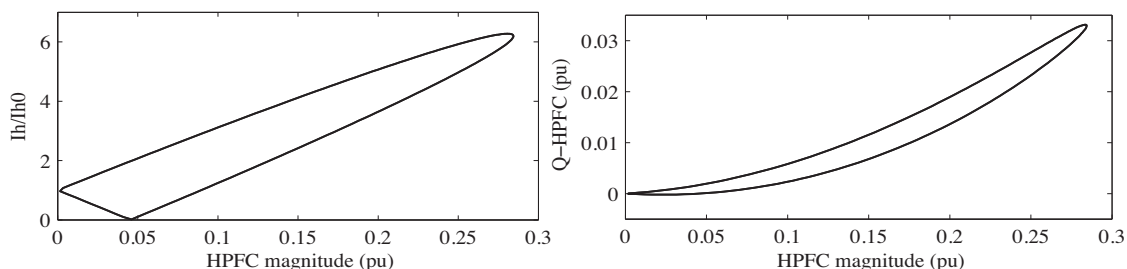


Figure 22. HPFC line harmonic current variation and HPFC harmonic reactive power versus HPFC value in ZAPI control method (I_0 is HPFC current before HPFC installation).

5. Simulation for a real network

The performance of the HPFC is evaluated in a real network, i.e. Iran north-west transmission system. Harmonic measurements have been performed at different locations in the Iran NW transmission system using HIOKI 3196 power quality analyzer. Figures 23 through 26 show the harmonic measurement at buses 1 through 4 for a one-day period with 10-min sampling intervals. As it can be seen, the 5th harmonic level is above IEEE 519 Std. limit (i.e. 1 %) during most of the measurement period. The objective in this case is to use an HPFC to change the harmonic impedance and accordingly alter harmonic flows such that the 5th harmonic level at bus 3 is decreased.

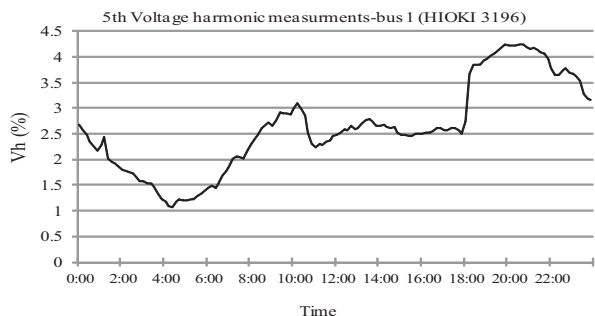


Figure 23. 5th harmonic voltage measurements at bus 1.

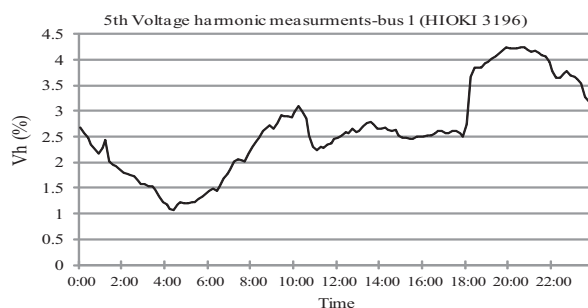


Figure 24. 5th harmonic voltage measurements at bus 2.

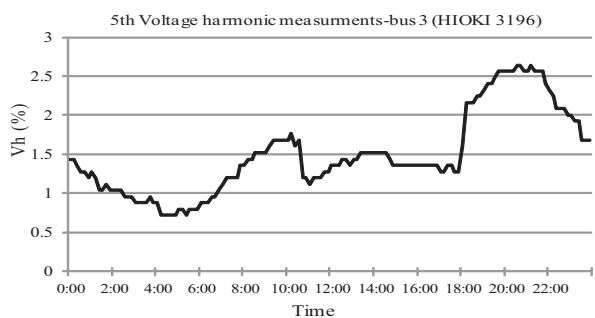


Figure 25. 5th harmonic voltage measurements at bus 3.

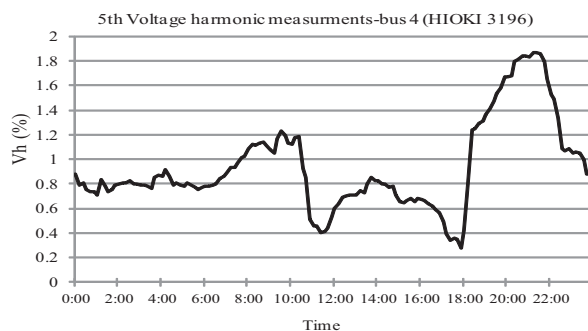


Figure 26. 5th harmonic voltage measurements at bus 4.

To design the HPFC, first the system model must be derived. The network is modeled at 400 kV and 230 kV voltage levels with 28 busbars (Figure 27). The harmonic voltage at busbar No. 3 is 4.3% which has caused complications in the network. To overcome the complications, the harmonic voltage needs to be decreased by a

factor of 1/2. In this regard, an HPFC is installed in line 2-4 and controlled using MAPI and ZAPI methods. HPFC system parameters are given in Table 2. The control settings and the HPFC capacity for each method are expressed in Table 3. As one can observe, the control schemes ZAPI and MAPI require 2.3 MVA and 1.63 MVA capacities for the HPFC, respectively. The effect of installing an HPFC in this line on the harmonic voltage at different busbars using these methods is depicted in Figure 28. It is evident that the harmonic voltage at busbar 3 is decreased by 50 % using both methods. Figure 28 also shows that at most of the busbars the 5th harmonic voltage is decreased.

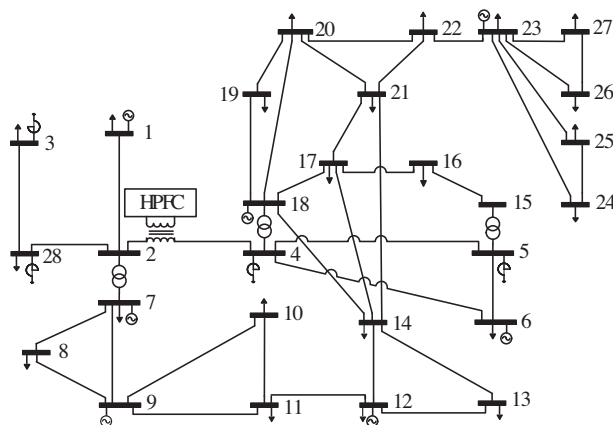


Figure 27. Iran north-west transmission system single-line diagram.

Table 2. HPFC parameters and rated values.

$S_{h,rated}(pu)$	$V_{rated}(kV)$	$V_{h,rated}(pu)$
0.05	400	0.05

Table 3. HPFC capacity and control settings using ZAPI and MAPI methods.

Method	$ V_{hpfc} (pu)$	$\angle V_{hpfc}(^{\circ})$	$Vh(3)/Vh0(3)$	$S_{hpfc}(pu)$	$Q_{hpfc}(pu)$	$P_{hpfc}(pu)$
ZAPI	0.0326	208	0.4979	0.0230	0.0230	0.0000
MAPI	0.032	36.9	0.5005	0.0163	0.0159	0.0036

6. Discussions

As one can see, the HPFC provides a new tool for the control of harmonic flow in a large and nonradial power system which may/may not have an active power exchange with the network. The use of an HPFC with/without active power exchange has to do with the size and performance of the HPFC. This concept can be compared to that of a DVR. In a DVR, different injection strategies may be employed. If the objective is to minimize the size of the DVR from the rating point of view, then the method of energy-minimized compensation is preferred. The drawback of this method is that there will be a phase-jump between the presag and postsag voltages which may not be desirable in the loads sensitive to the supply phase. In the energy-minimized compensation control of a DVR, no active power is exchanged between the DVR and the network. However, if the objective is to compensate the sag such that the load will not see a phase-jump, then the method of presag compensation is preferred. The trade-off of this method is the size of the DVR and active-power exchange between the DVR

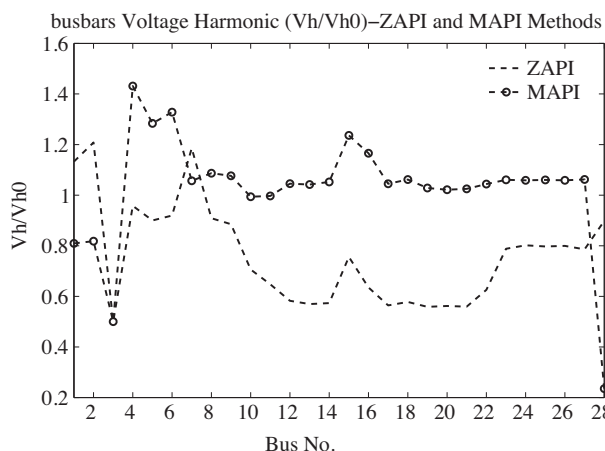


Figure 28. Ratio of harmonic voltage at Iran north-west busbars after installation of an HPFC in line 2-4 with ZAPI and MAPI control methods.

and the network [21, 22]. The same concept also applies here. If the harmonic objective function is to be achieved with an HPFC of minimum rating, then the trade-off is the need of power storage component. If one prefers not to have an energy storage, then an HPFC with a higher rating must be used. It is clear that a cost optimization-strategy may also be needed to be explored. Similar to the presag/in-phase control of a DVR, an HPFC can be controlled in such a way that an active power is exchanged between the HPFC and the system. Note that in the case of an HPFC, the injected voltage is a harmonic term, and therefore, the exchange of power occurs at a harmonic frequency. In this case, the size of the HPFC may be minimum, but the dc link of the HPFC needs to have an energy storage system. If an HPFC is controlled such that no active power is exchanged between the HPFC and the grid, no energy storage system or no extra VSC is required. This can be compared to the energy-minimized compensation method of a DVR. In this method, no energy storage is needed, but the size of the HPFC is not minimal. Although in the current manuscript, the performance of the HPFC is evaluated based on an open-loop control strategy, the HPFC can also be equipped with a control system which enables harmonic flow in nonstationary harmonic environments. If the harmonic profile of the network is of fast changing behavior, then to achieve the best solution is to have closed loop control algorithm. If the harmonic profile does not change rapidly, then an open-loop strategy can be a better and cheaper solution. It is worth nothing that closed-loop control of an HPFC (or a network of several HPFCs) may require data transfer from different locations in a power system.

In this manuscript, the performance of one HPFC at a specific location is studied. In practice, the location of the HPFC as well as the magnitude and the angle of the injected voltage can be optimally selected to achieve the best results. It may also visible to use more than one HPFC in a power network to achieve the best harmonic environment. Therefore, the problem looks like a multilateral one, which requires an optimization with respect to several parameters.

7. Conclusion

In this paper, a novel method for the control of harmonics at a system level is proposed. The harmonic levels in MV/HV systems, which are due to inefficient filtering at load sides or possible harmonic resonances, are reduced by controlling the harmonic flow in the system. The flow control is performed by using a conventional series active power filter, but controlled with a different strategy. The active filter which controls the harmonic power

(current) flow in the network is named HPFC. By using the HPFC, harmonic voltages can be controlled by redirecting harmonic power (current) in the network. The HPFC is a device similar to a DVR, which is installed in series with the network elements such as lines, transformers, capacitors, filters and generators. The HPFC regulates the harmonic current flow in these elements by injecting a series harmonic voltage. In this paper, two local control methods based on local parameters, namely MAPI and ZAPI, are proposed. Simulation results show that in the MAPI control method, the HPFC rated capacity will be minimal, and the active power exchange between the HPFC and network will be negligible by the ZAPI control method. To show the applicability of the proposed harmonic control method, an HPFC is designed for a real case, i.e. Iran NW transmission system. Harmonic measurements show a high level of the 5th harmonic in this system. It is shown that designing an appropriate HPFC for Iran NW transmission system can effectively reduce the harmonic levels.

8. Future works

The main objective of this paper in this very first work is to open a new chapter of harmonic mitigation studies based on a new idea of harmonic-flow control by injecting harmonic signals into a network. This conceptual introduction assumes only one HPFC at one location in a stationary harmonic environment. However, many new ideas arise following this introduction some of which are summarized below. Since the place of the HPFC as well as the magnitude/angle of the injected signal can change the performance of the overall system, one can define a cost function composed of these three parameters, i.e. location of the HPFC, magnitude and angle of the injected signal. Minimizing this cost function can result in a more harmonic standard compliant system. One can also propose to use more than one HPFC or use of several HPFCs with lower ratings at different locations in a power network to come up with a better harmonic situation. Having said that, a new chapter of locating optimization arises. This issue along with the fact that it is preferred to use a minimum no. of HPFC devices to reduce the costs brings up a new chapter of determining a minimum no. of HPFCs at optimal locations which result in the best harmonic situation from standards point of view. If the harmonic profile of the network is of fast changing behavior, then to achieve the best solution is to have closed loop control algorithm. Therefore, one future work would be to design a closed-loop harmonic control system which, of course, is a challenging issue due to the fact that the reference signals are not of dc type. Although, this paper introduces the application of HPFC for just one harmonic, the concept can be further extended to more than one harmonic. This matter brings up several all the other concerns explained above.

Acknowledgment

The authors would like to thank the other members of Power Quality Lab at Sharif University of Technology, Farhad Pourtahmasbi, Behnam Akbari, and Mehdi Naghdi, for providing detailed measurement data and analysis.

References

- [1] Abu-Hashim R, Burch R, Chang G, Grady M, Gunther E et al. Test systems for harmonics modeling and simulation. *IEEE Transactions on Power Delivery* 1999; 14 (2): 579-587. doi: 10.1109/61.754106
- [2] Fujita H, Akagi H. A practical approach to harmonic compensation in power systems-series connection of passive and active filters. *IEEE Transactions on Industry Applications* 1991; 27(6): 1020-1025. doi: 10.1109/28.108451
- [3] Figueroa D, Moran L, Ruminot P, Dixon J. A series active power filter scheme for current harmonic compensation. In: 2008 IEEE PES Power Electronics Specialists Conference; Rhodes, Greece; 2008. pp. 3587-3591.

- [4] Ribeiro E, Barbi I. A series active power filter for harmonic voltage suppression. In: Twenty-third International Telecommunications Energy Conference; Edinburgh, UK; 2001. pp. 514-519.
- [5] Jianjun G, Dianguo X, Hankui L, Maozhong G. Unified power quality conditioner (UPQC): the principle, control and application. In: Proceedings of the Power Conversion Conference; Osaka, Japan; 2002. pp. 80-85.
- [6] Tey L, So P, Chu Y. Improvement of power quality using adaptive shunt active filter. *IEEE Transactions on Power Delivery* 2005; 20 (2): 1558-1568. doi: 10.1109/TPWRD.2004.838641
- [7] Bhim S, Ritankar S, Kamal H. Static synchronous compensator (STATCOM): a review. *IET Power Electronics* 2009; 2 (4): 297-324. doi: 10.1049/iet-pel.2008.0034
- [8] Kiran B, Pradip C. Power conditioner for Voltage Sag/Swell and Harmonic Mitigation. In: 2019 IEEE International Conference on Electrical, Computer and Communication Technologies; Coimbatore, India; 2019. pp.63-69.
- [9] He J, Du L, Yuan S, Zhang C, Wang C. Supply voltage and grid current harmonics compensation using multi-port interfacing converter integrated into Two-AC-Bus Grid. *IEEE Transactions on Smart Grid* 2019; 10 (3): 3057-3070. doi: 10.1109/TSG.2018.2817491
- [10] Hosseini S, Banaei M. A new minimal energy control of the DC link energy in four-wire dynamic voltage restorer. In: 30th Annual Conference of IEEE Industrial Electronics Society; Busan, South Korea; 2004. pp.3048-3053.
- [11] Carpinelli G, Russo A, Varilone P. Active filters: A multi-objective approach for the optimal allocation and sizing in distribution networks. In: International Symposium on Power Electronics, Electrical Drives, Automation and Motion; Ischia, Italy; 2014. pp. 1201-1207.
- [12] Han XM, You Y, Liu H. Principle and realization of a dynamic voltage regulator (DVR) based on line voltage compensating. In: Proceedings of the Chinese Society of Electrical Engineering; China; 2003. pp.49-53.
- [13] IEEE Recommended Practice for Establishing Liquid-Filled and Dry-Type Power Distribution Transformer Capability When Supplying Nonsinusoidal Load Currents. *IEEE Standard C57.110-2008* 2008; pp.c1-44.
- [14] Yildirim D, Fuchs E. Measured transformer derating and comparison with harmonic loss factor (FHL) approach. *IEEE Transactions on Power Delivery* 2000; 15 (1):186-191. doi: 10.1109/61.847249
- [15] Shun T, Xiangning X. Comparing transformer derating computed using the harmonic loss factor FHL and K-factor. In: Third International Conference on Electric Utility Deregulation and Restructuring and Power Technologies; Nanjing, China; 2008. pp.1631-1634.
- [16] Sumaryadi GH, Suslilo A. Effect of power system harmonic on degradation process of transformer insulation system. In: IEEE 9th International Conference on the Properties and Applications of Dielectric Materials; Harbin, China; 2009. pp.261-264.
- [17] Pei L, Guodong L, Yonghai X, Shujun Y. Methods comparison and simulation of transformer harmonic losses. In: 2010 Asia-Pacific Power and Energy Engineering Conference; Chengdu, China; 2010. pp.238-241.
- [18] Ghosh A, Ledwich G. Structures and control of a Dynamic Voltage Regulator (DVR). In: Power Engineering Society Winter Meeting 2001; Ohio, USA. pp. 1027-1032.
- [19] Rakesh G, Vimala Kumar K. Performance improvement of DVR by control of reduced-rating with a battery energy storage system. In: IEEE International Conference on Power, Control, Signals and Instrumentation Engineering (ICPCSI); Chennai, India; 2017. pp.1897-1904.